The KARMEN final results on the search for $\bar{\nu}_e$ from μ^+ decay at rest

Klaus Eitel

Institut für Kernphysik, Forschungszentrum Karlsruhe, 76021 Karlsruhe, Germany

Abstract. We review the search for $\bar{\nu}_e$ from μ^+ decays at rest with the KARMEN experiment. A potential excess of $\bar{\nu}_e$-induced events as seen in the LSND experiment can be interpreted as evidence for $\bar{\nu}_\mu \to \bar{\nu}_e$ or as indication of lepton flavor (LF) violation in μ^+ decays. The KARMEN results show no hint for extra $\bar{\nu}_e$, thereby excluding large parameter areas for an oscillation signal as well as the LF violating μ^+ decay at more 90% C.L. as source of the LSND $\bar{\nu}_e$ excess.

In the last years, tremendous progress has been achieved to firmly establish the nature of neutrino oscillations using neutrinos from the sun as well as neutrinos produced in the earth's atmosphere. However, with oscillation parameters accessible to accelerator based experiments, the situation remains unsettled. There is one evidence for oscillations in the appearance mode $\bar{\nu}_\mu \to \bar{\nu}_e$ from the LSND experiment [1] which is in contrast to results from the KARMEN experiment, but also partly excluded by accelerator-based experiments such as NOMAD [2] and NuTeV [3]. In this paper, we summarize the results of the KARMEN search for appearance of $\bar{\nu}_e$ within a very pure $\bar{\nu}_\mu$ flux from μ^+ decays at rest (DAR) indicating either the flavor oscillation $\bar{\nu}_\mu \to \bar{\nu}_e$ or other non-SM processes, e.g. lepton family number violating μ^+ decays $\mu^+ \to e^+ + \bar{\nu}_e + (\bar{\nu})$.

EXPERIMENTAL CONFIGURATION AND DATA REDUCTION

The experiment was performed at the neutrino source of the ISIS synchrotron accelerating protons to an energy of 800 MeV before striking a massive beam stop target. Neutrinos emerge isotropically from the consecutive decays at rest (DAR) $\pi^+ \to \mu^+ + \nu_\mu$ and $\mu^+ \to e^+ + \nu_e + \bar{\nu}_\mu$ assuming the ν–flavors of the SM decay channels. Neutrinos from μ^+ DAR have a continuous energy spectrum up to 52.83 MeV. Due to the narrow time structure of 525 ns of the proton pulses muons are produced in a short time window compared to their lifetime of 2.2 μs.

The neutrinos are detected in a 56 t scintillation calorimeter [4] at a mean distance of 17.6 m from the ISIS target (fig. 1). The calorimeter is a mineral oil based scintillator segmented into 512 independent modules. Gadolinium within the module walls allows effective neutron detection via Gd(n,γ) with on average 3 γ's of energy $\sum E_\gamma = 8$ MeV in addition to the capture on the hydrogen of the scintillator via p(n,γ). The scintillation detector provides an almost pure target of ^{12}C and ^{1}H for ν-interactions. Three veto layers ensure a search for LF violating μ^+ decays almost free of cosmic background.

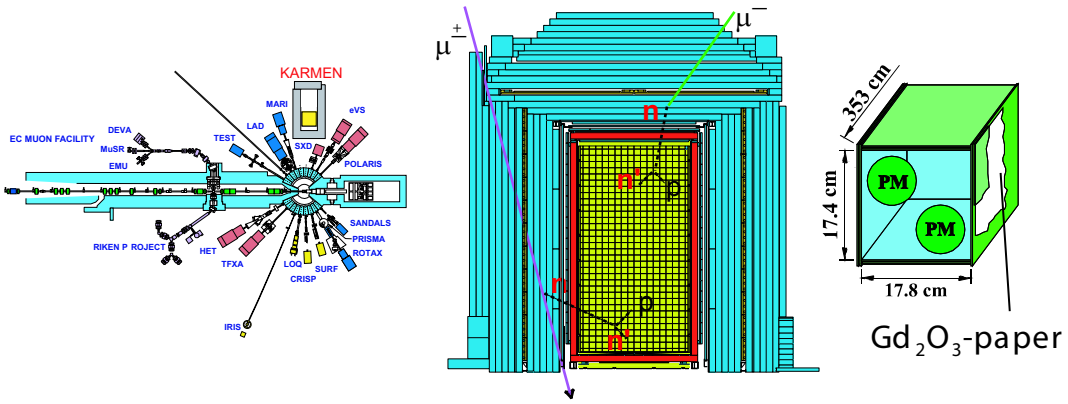

FIGURE 1. *Schematic view of the KARMEN detector located at the ISIS target; front view of detector tank with its layers of active vetos and the passive iron shielding; cross section of an individual scintillator module with the photomultiplier pair at each module end.*

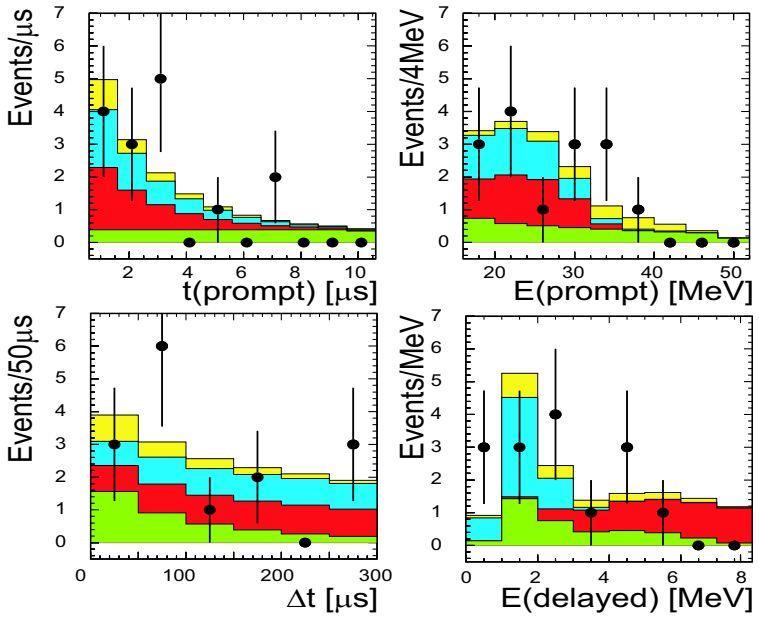

FIGURE 2. *KARMEN 15 coincidence candidates after final cuts.*

After a substantial upgrade consisting of a third active muon veto system of 300 m^2 plastic scintillators to reduce cosmic induced neutron background [5], the KARMEN 2 experiment took data from February 1997 to March 2001. During this time, protons equivalent to a total charge of 9425 Coulombs have been accumulated on the ISIS target.

A $\bar{\nu}_e$ signal consists of a spatially correlated delayed (e^+,n) sequence. The requirements for event sequences in KARMEN are described in detail in [6] and references therein. Applying all cuts to the data, 15 (e^+,n) candidate sequences were finally reduced. Figure 2 shows the remaining sequences in the appropriate energy and time windows. The background components are also given with their distributions. The expected

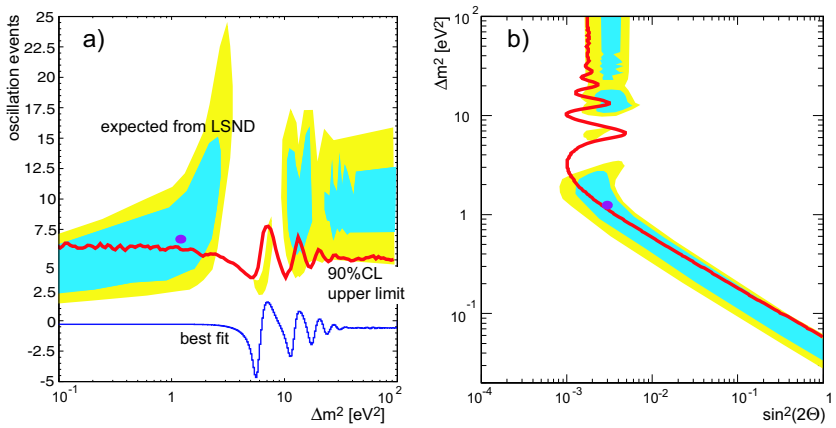

FIGURE 3. *(a) KARMEN limit and expected event rate following the LSND signal strength. (b) oscillation plot with LSND favored regions and KARMEN exclusion curve. The dot denotes the LSND best fit values.*

background amounts to 15.8 ± 0.5 events. This number comprises 3.9 ± 0.2 events from cosmic induced sequences as well as ν induced reactions such as intrinsic source contamination of $\bar{\nu}_e$ (2.0 ± 0.2), ν_e induced random coincidences (4.8 ± 0.3) and (e^-,e^+) sequences from $^{12}\mathrm{C}\,(\,\nu_e\,,\mathrm{e}^-\,)\,^{12}\mathrm{N}_{\mathrm{g.s.}}$ with subsequent ^{12}N decay (5.1 ± 0.2). Except for the intrinsic $\bar{\nu}_e$ contamination, deduced from detailed MC simulations, all the background components have been measured in different time and energy regimes with the KARMEN detector and extrapolated into the evaluation cuts applied for the $\bar{\nu}_e$ search. The extracted number of sequences is in excellent agreement with the background expectation, consistent with no additional $\bar{\nu}_e$ signal.

LIMITS ON NEUTRINO OSCILLATIONS $\bar{\nu}_\mu \rightarrow \bar{\nu}_e$

To analyze the extracted sequences with respect to a potential contribution of $\bar{\nu}_e$ from oscillations $\bar{\nu}_\mu \rightarrow \bar{\nu}_e$, an event-based maximum likelihood method is applied. This method includes the detailed spectral information of each individual event as well as the expected event parameters for a specific oscillation hypothesis with the free parameters Δm^2 and the oscillation amplitude, usually expressed in the simplified 2-dim scheme as $\sin^2(2\Theta)$. Fig. 3(a) shows the results of this analysis in terms of oscillation events as function of Δm^2. The best fit line is compatible with zero. Applying a unified frequentist approach [7] leads to the given 90% C.L. upper limit which can be compared to what one would expect as signal strength in KARMEN taken the evidence from LSND. These KARMEN results are in clear contrast to the LSND evidence. However, KARMEN does not rule out completely the parameters favored by LSND. Therefore, two problems have to be addressed: What is the level of compatibility of both experiments? Assuming statistical compatibility, what are the oscillation parameters accepted by both experiments? A detailed combined statistical analysis [8] based on an earlier study with intermediate data sets [9] has been performed to answer these questions. To summarize, LSND and KARMEN are incompatible at a level of 36 % confidence. Assuming statistical com-

patibility, all parameter combinations with $\Delta m^2 > 1\,\mathrm{eV}^2$ are excluded apart from a little 'island' at $\approx 7\,\mathrm{eV}^2$.

LIMITS ON LF VIOLATING μ^+ DECAYS

The LF number violating decay mode $\mu^+ \to e^+ + \bar{\nu}_e + (\bar{\nu})$ is allowed in many extensions of the SM, e.g. the decay mode $\mu^+ \to e^+ + \bar{\nu}_e + \nu_\mu$ in left–right (LR) symmetric models [11], supersymmetric models with R parity violation [12], or the decay mode $\mu^+ \to e^+ + \bar{\nu}_e + \bar{\nu}$ in extensions involving additional scalar multiplets [13] (fig. 4). With the rest masses much smaller than the energy of all neutrinos emitted in $\mu^+ \to e^+ + \bar{\nu}_e + (\bar{\nu})$, an analytical description of the neutrino spectra similar to the SM one can be applied, with the spectral parameter $\tilde{\rho}$ to be specified, replacing the SM Michel parameter ρ.

Although the energy scale of LR symmetry of weak interactions or the appearance of supersymmetric particles is expected to be in the range of 0.1–1 TeV, these extensions could manifest in small branching ratios at energy scales of muon decays at rest and lead to an excess of $\bar{\nu}_e$-induced events compared to SM predictions, i.e. explain the $\bar{\nu}_e$ signal seen by LSND. For details of the KARMEN analysis towards such μ^+ decays, we refer to [10].

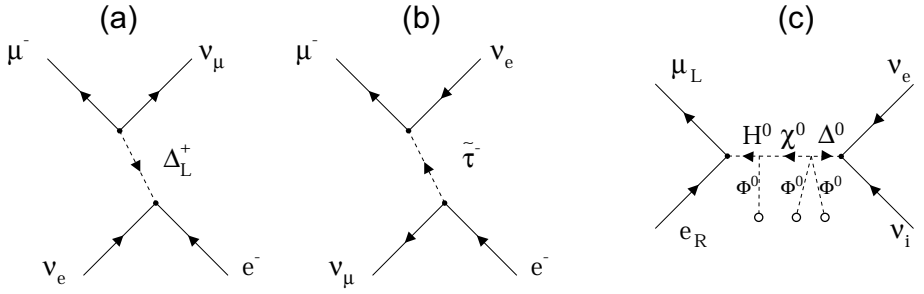

FIGURE 4. LF violating μ^+ decays in different extensions of the SM, with the exchange of (a) charged Higgs triplet fields [11] in left-right symmetric models, (b) supersymmetric partners of the τ lepton [12] in Supersymmetry or (c) scalar multiplets [13]

Figure 5 shows the prompt energy of the 15 reduced sequences together with the results of the maximum likelihood analysis for different kinematical parameters $\tilde{\rho}$ (as expected for models [11] or [13]) for the emitted $\bar{\nu}_e$. Table 1 shows the results of the likelihood method. They are consistent with no $\bar{\nu}_e$ emission from μ^+ decay with upper limits extracted within a unified frequentist analysis near the physical boundary N($\bar{\nu}_e$)=0 following [7]. The above limits on the branching ratio *BR* on μ^+ decays emitting $\bar{\nu}_e$ improve by more than an order of magnitude the most sensitive limit so far of $BR(\mu^+ \to e^+ + \bar{\nu}_e + \nu_\mu) < 0.012$ obtained by the E645 experiment at LAMPF [14]. The most conservative upper limit of $BR < 1.7 \cdot 10^{-3}$ for any parameter $\tilde{\rho}$ is also in direct experimental disagreement with the possibility that the beam excess of $\bar{\nu}_e$ seen in the LSND experiment with a branching ratio or probability of $P = (2.64 \pm 0.67 \pm 0.45) \cdot 10^{-3}$ [1] is due to μ^+ decays with $\bar{\nu}_e$ emission.

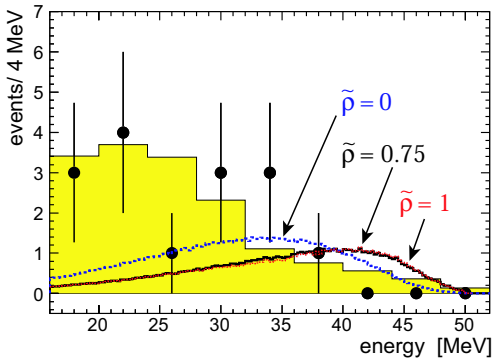

FIGURE 5. Visible energy distribution of candidate events with background expectation (shaded area). The lines show the 90% C.L. limit for an additional $\bar{\nu}_e$ signal with different spectral parameters $\tilde{\rho}$.

TABLE 1. Flux averaged cross section $\langle\sigma\rangle$ for $\mathrm{p}(\bar{\nu}_e, \mathrm{e}^+)\mathrm{n}$ and $^{12}\mathrm{C}(\bar{\nu}_e, \mathrm{e}^+\mathrm{n})^{11}\mathrm{B}$, expected (e^+, n) sequences for μ^+ decaying entirely via $\mu^+ \to \mathrm{e}^+ + \bar{\nu}_e + (\bar{\nu})$, experimental results for potential $\bar{\nu}_e$-induced events and deduced upper limits for the branching ratio.

$\tilde{\rho}$	$\langle\sigma\rangle[10^{-42}\mathrm{cm}^2]$		$\mathrm{N}(\bar{\nu}_e)_{\mathrm{BR}=1}$	$\mathrm{N}(\bar{\nu}_e)_{\mathrm{bestfit}}$	$\mathrm{N}(\bar{\nu}_e)_{90\%\mathrm{CL}}$	BR (90% C.L.)
	$\bar{\nu}_e + p$	$\bar{\nu}_e + {}^{12}\mathrm{C}$				
0.0	72.0	4.5	4304 ± 403	$+0.3$	< 7.1	$< 1.7 \cdot 10^{-3}$
0.25	78.8	5.8	4773 ± 445	-0.1	< 6.2	$< 1.3 \cdot 10^{-3}$
0.5	86.0	7.2	5273 ± 489	-0.4	< 6.0	$< 1.1 \cdot 10^{-3}$
0.75	93.5	8.5	5828 ± 538	-0.8	< 5.3	$< 0.9 \cdot 10^{-3}$

The data presented here are the results of years of experimental work and data analysis. I am deeply indebted to all the colleagues of the KARMEN collaboration for their expertise and enthusiasm in running a long term experiment successfully. It is a great pleasure to thank the organizers of the CIPANP conference, especially the coordinators of an exciting session on neutrinos, Bruce Berger and Bonnie Fleming, for a very stimulating and interesting meeting.

REFERENCES

1. A. Aguilar *et al.*, Phys. Rev. D **64**, 112007 (2001).
2. P. Astier *et al.*, `hep-ex/0306037`.
3. S. Avvakumov *et al.*, Phys. Rev. Lett. **89**, 011804 (2002).
4. G. Drexlin *et al.*, Nucl. Instrum. Methods A **289**, 490 (1990).
5. G. Drexlin, Prog. Part. Nucl. Phys. **40**, 193 (1998).
6. B. Armbruster *et al.*, Phys. Rev. D **65**, 112001 (2002).
7. G.J. Feldman and R.D. Cousins, Phys. Rev. D **57**, 3873 (1998).
8. E. Church *et al.*, Phys. Rev. D **66**, 013001 (2002).
9. K. Eitel, New Jour. Phys. **2**, 1.1 (2000).
10. B. Armbruster *et al.*, Phys. Rev. Lett. **90**, 181804 (2003).
11. P. Herczeg and R.N. Mohapatra, Phys. Rev. Lett **69**, 2475 (1992).
12. A. Halprin and A. Masiero, Phys. Rev. D **48**, R2987 (1993).
13. K.S. Babu and S. Pakvasa, `arXiv:hep-ph/0204236`.
14. K. Hagiwara et al., Phys. Rev. D **66**, 010001 (2002).